

Cell autonomous regulation of herpes and influenza virus infection by the circadian clock

Rachel S. Edgar^a, Alessandra Stangherlin^a, Andras D. Nagy^{a,b}, Michael P. Nicoll^{c,1}, Stacey Efstathiou^{c,1}, John S. O'Neill^{a,2}, and Akhilesh B. Reddy^{a,3}

^aUniversity of Cambridge Metabolic Research Laboratories, Wellcome Trust-Medical Research Council Institute of Metabolic Science, University of Cambridge, Addenbrooke's Hospital, Cambridge CB2 0QQ, United Kingdom; ^bDepartment of Anatomy, University of Pecs Medical School, H-7624 Pecs, Hungary; and ^cDivision of Virology, Department of Pathology, University of Cambridge, Cambridge CB2 1QP, United Kingdom

Edited by Joseph S. Takahashi, Howard Hughes Medical Institute, University of Texas Southwestern Medical Center, Dallas, TX, and approved July 6, 2016 (received for review February 3, 2016)

Viruses are intracellular pathogens that hijack host cell machinery and resources to replicate. Rather than being constant, host physiology is rhythmic, undergoing circadian (~24 h) oscillations in many virus-relevant pathways, but whether daily rhythms impact on viral replication is unknown. We find that the time of day of host infection regulates virus progression in live mice and individual cells. Furthermore, we demonstrate that herpes and influenza A virus infections are enhanced when host circadian rhythms are abolished by disrupting the key clock gene transcription factor *Bmal1*. Intracellular trafficking, biosynthetic processes, protein synthesis, and chromatin assembly all contribute to circadian regulation of virus infection. Moreover, herpesviruses differentially target components of the molecular circadian clockwork. Our work demonstrates that viruses exploit the clockwork for their own gain and that the clock represents a novel target for modulating viral replication that extends beyond any single family of these ubiquitous pathogens.

circadian | clock | virus | herpes | influenza

Diverse behavioral, physiological, and cellular processes exhibit daily (circadian) rhythms, which persist without external timing cues. Cell autonomous biological clocks drive circadian rhythms observed at the whole organism level, enabling adaptation to the 24-h cycle produced by the Earth's rotation (1). At the molecular level, circadian oscillations are thought to be generated by genetic feedback loops involving the activating transcription factors BMAL1 (ARNTL/Mop3), NPAS, and CLOCK. These drive transcription of repressor proteins CRYPTOCHROME1/2 (CRY1/2) and PERIOD1/2 (PER1/2) that feedback to repress their own transcription, additionally regulated by myriad post-translational processes (2–4).

Circadian clocks confer competitive advantages to organisms. Their disruption incurs fitness costs, and they influence many aspects of human health and disease including sleep/wake cycles and immune function (5, 6). Indeed, many innate and adaptive immune responses are clock regulated. The immune response undergoes regeneration and repair as the host transitions to the resting phase of the daily cycle, but is primed for pathogen attack at the onset of the active phase (5, 6). Although changes in host responses to bacterial endotoxin or infection at different times of day have been reported (7, 8), the influence of host circadian clocks on progression of viral diseases is unknown. Here, we demonstrate dynamic host–virus interactions over the 24-h day and also show that genetic clock disruption augments virus replication in mice and cells.

Results

Viruses are obligate intracellular pathogens and require host organisms to proliferate. Over the course of a day, viruses may encounter host environments that are more or less conducive to replication and dissemination (5, 9, 10). We hypothesized that the time of day of infection would influence viral replication. To

test this, we infected WT mice intranasally with a recombinant *luciferase*-expressing virus, Murid Herpesvirus 4 (*M3:luc* MuHV-4), at two times of day (Fig. 1A and Fig. S1A). As a rodent pathogen, this virus elicits natural host immune responses and implements evasion strategies in laboratory mice (11, 12), which allow it to establish latent (or quiescent) infection after primary infection. WT mice infected intranasally at the onset of resting phase [Zeitgeber Time 0 (ZT0); lights on], exhibited 10-fold higher viral replication than mice infected just before their active phase (ZT10) (Fig. 1A). This time-of-day effect required a functional clock because *Bmal1*^{−/−} mice, which have no overt circadian rhythms (2), showed no difference when infected at different times (Fig. 1B and Fig. S1B). Furthermore, *Bmal1*^{−/−} mice exhibited high levels of MuHV-4 infection when inoculated at either time of day (Fig. S1C–F). Together, these results indicate that the timing of infection in relation to the circadian cycle has major effects on herpesvirus pathogenesis.

Because infection of *Bmal1*^{−/−} mice resulted in high levels of virus replication in vivo (Fig. S1D and F), we hypothesized that its role in clock function was important in regulating virus propagation. We therefore tracked *M3:luc* MuHV-4 infection longitudinally in WT and *Bmal1*^{−/−} mice, infecting intranasally at ZT7: the time when BMAL1 is maximally active at genomic sites in peripheral tissues (9). Strikingly, virus replication increased

Significance

The circadian clock coordinates our physiology. Circadian disruption, as occurs during shift work, increases the risk of chronic diseases. For infectious diseases, circadian regulation of systemic immunity seems to underpin “time-of-day” differences in responses to extracellular pathogens. However, circadian rhythms are cell autonomous, and their interaction with intracellular pathogens, such as viruses, is poorly understood. We demonstrate that time of day of virus infection has a major impact on disease progression, in cellular models as well as in animals, highlighting the key role that cellular clocks play in this phenomenon. Clock disruption leads to increased virus replication and dissemination, indicating that severity of acute infections is influenced by circadian timekeeping.

Author contributions: R.S.E. and A.B.R. designed research; R.S.E., A.S., A.D.N., M.P.N., and J.S.O. performed research; M.P.N. and S.E. contributed new reagents/analytic tools; R.S.E., A.S., A.D.N., M.P.N., S.E., J.S.O., and A.B.R. analyzed data; and R.S.E. and A.B.R. wrote the paper.

The authors declare no conflict of interest.

This article is a PNAS Direct Submission.

¹Present address: Division of Virology, National Institute for Biological Standards and Control, Hertfordshire EN6 3QG, United Kingdom.

²Present address: Cell Biology Division, MRC Laboratory of Molecular Biology, Cambridge CB2 0QH, United Kingdom.

³To whom correspondence should be addressed. Email: areddy@cantab.net.

This article contains supporting information online at www.pnas.org/lookup/suppl/doi:10.1073/pnas.1601895113/-DCSupplemental.

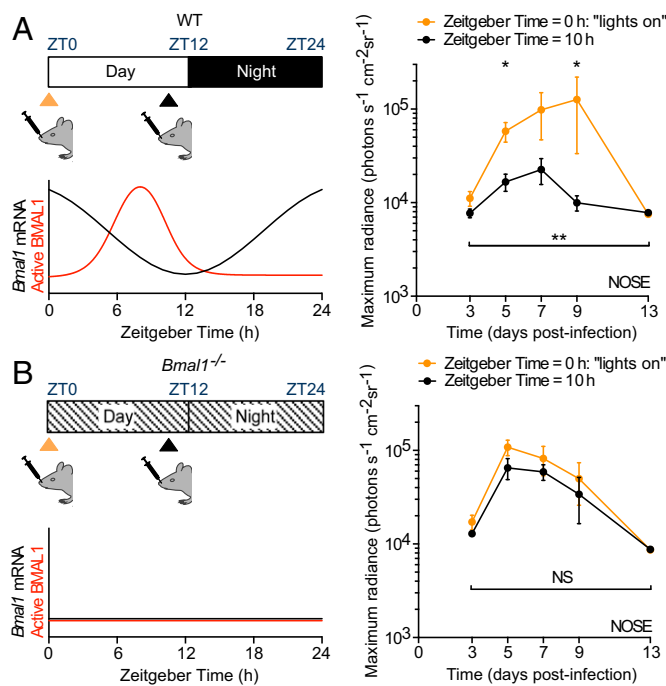


Fig. 1. Herpesvirus infection in mice is regulated by the circadian clock. (A) WT female mice were intranasally infected with *M3:luciferase* Murid Herpesvirus 4 (*M3:luc* MuHV-4) at Zeitgeber Time 0 (ZT0) (lights on; $n = 6$) or at ZT10 ($n = 6$). Schematic illustrates *Bmal1* mRNA levels and active (genome-bound) BMAL1 protein over the day and night. Infection was monitored by bioluminescence imaging. Primary infection in the nose is higher in mice inoculated at the onset of the resting phase (ZT0) compared with infection before the active phase (ZT10) [mean \pm SEM; two-way ANOVA (ZT of infection \times time postinfection): ZT of infection effect, $P = 0.0021$; post hoc t tests, $*P < 0.05$]. See also Fig. S1A. (B) Female *Bmal1*^{-/-} mice were infected with *M3:luc* MuHV-4 at either ZT0 ($n = 5$) or ZT10 ($n = 6$) and infection monitored as for A [mean \pm SEM; two-way ANOVA (ZT of infection \times time postinfection): ZT of infection effect, $P > 0.05$; NS = not significant]. See also Fig. S1B.

greater than threefold at days 5–7 in *Bmal1*^{-/-} mice compared with WT mice (Fig. 2A and B and Fig. S24). We saw a similar pattern when the acute infection spread to the superficial cervical lymph nodes (SCLNs) (Fig. 2A and B). By contrast, latent infection was established to a similar extent in WT and *Bmal1*^{-/-} mice (Fig. S2B and C).

To exclude that elevated infection levels were specific to MuHV-4, we infected mice with a different herpesvirus, herpes simplex virus 1 (HSV-1), by scarification of the left ear. We tracked the progression and extent of HSV-1 infection using a recombinant virus encoding *luciferase* under the control of the cytomegalovirus immediate early gene promoter (*CMV:luc* HSV-1) (13). Acute HSV-1 infection was significantly enhanced in arrhythmic *Bmal1*^{-/-} mice (Fig. 2C and D and Fig. S2D and E), as with MuHV-4. As infection progressed, *Bmal1*^{-/-} mice failed to contain HSV-1 spread, which disseminated across the head to the right ear (Fig. 2C and D). As with MuHV-4, although acute infection was more severe when circadian rhythms were disrupted, latent infection was established to a similar extent in both genotypes. Although apparent trends toward higher numbers of latent viral genomes in *Bmal1*^{-/-} mice was noted, this did not reach statistical significance (Fig. S2F), suggesting that circadian rhythms principally modulate primary infection in vivo.

A more vigorous immune response to incoming virus at the onset of the active phase might oppose MuHV-4 infection at ZT10 in vivo. We therefore investigated virus replication at different circadian times in synchronized cell models, which display robust ~ 24 -h rhythms but are not subject to systemic immune

regulation (Fig. 3A). For our in vitro cellular clock model, we used confluent monolayers in which there were limited numbers of dividing cells, and no detectable circadian rhythm in cell cycle activity after synchronization (Fig. S3 and Movie S1). We used high resolution real-time bioluminescence recording to monitor both *M3:luc* MuHV-4 replication kinetics and the amount of virus replication (measured by total bioluminescence) correlated with infectious particle production (Fig. 3B and Fig. S4A–C). Strikingly, when cell populations were infected with MuHV4 at different times in vitro, the time-of-day effect on infection observed in mice was recapitulated (Fig. 3C and D). Total bioluminescence was significantly increased in cells infected during the rising phase of *Bmal1* expression (CT18–24, indicated by open arrowheads) compared with cells infected during decline of *Bmal1* expression (CT30–36, indicated by solid arrowheads) (Fig. 3C). Moreover, MuHV-4 infection at different times significantly altered the rate of virus replication (Fig. 3D). Indeed, the entire kinetic profile of infection depended on the circadian phase the virus encountered, such that slower initial replication rates were associated with prolonged viral gene expression [Fig. 3D and Fig. S4D; Pearson's $r = 0.999$ (first cycle) or $r = 0.982$ (second cycle), $P < 0.01$].

Moreover, in agreement with our in vivo observations, MuHV-4 infection was significantly increased in primary *Bmal1*^{-/-} fibroblasts compared with WT cells (Fig. 4A and B and Movie S2). When synchronized WT and *Bmal1*^{-/-} fibroblasts were infected at different circadian times (Fig. S5A; CT of infection indicated by open and solid arrowheads), the time-of-day effect on MuHV-4 infection in WT cells was abolished in those from *Bmal1*^{-/-} mice (Fig. 4C and Fig. S5B). Additionally, HSV-1 replication was significantly enhanced in *Bmal1*^{-/-} cells compared with WT cells (Fig. 4D and E and Movie S3). Thus, the cellular circadian clock exerts a major effect on herpesvirus infection, indicating that our observations in live mice do not simply result from circadian modulation of immune cell function.

Given that cellular circadian rhythms impact on virus replication, we speculated that herpesviruses may manipulate the molecular clockwork during infection. To assess this, we infected mouse NIH 3T3 cells, expressing luciferase under the control of the *Bmal1* promoter (*Bmal:luc*), with MuHV-4 at different circadian times (Fig. 5A and Fig. S64). Interestingly, MuHV-4 acutely induced *Bmal1* expression from ~ 6 h after infection, irrespective of the circadian phase at which the cells were infected (one-way ANOVA: peak *Bmal:luc*, $P < 0.0001$). The subsequent cellular circadian rhythms during viral infection depended on the time at which cells were infected. Virus-mediated *Bmal1* induction during the endogenous fall in *Bmal1* transcription generated a *Bmal1* peak and disrupted circadian reporter expression (infection at CT18–24, indicated by open arrowhead in Fig. 5A and Fig. S5). In contrast, viral induction at other times (infection at CT30–36; indicated by solid arrowhead in Fig. 5A) enhanced the usual rise in *Bmal1* transcription, and cellular rhythms remained robust for three cycles afterward (Fig. S64). These findings strongly suggest that induction of *Bmal1* expression by herpesviruses has different consequences for clock function depending on when in the circadian cycle infection occurs.

Analogous to arrhythmic *Bmal1*^{-/-} in vivo and cellular models, enhanced viral replication was observed in cells infected at circadian times when endogenous circadian rhythms were subsequently disrupted (Figs. 3D and E and 5A and B; indicated by open arrowheads). In mouse peripheral tissues that support herpesvirus replication, cellular CT24 corresponds to onset of the rest (light) period (14), where rapid, higher levels of initial replication would maximize the chance of transmission during the subsequent active (dark) phase 12–24 h later. Cellular CT36 corresponds to the onset of the active period, when slower, lower levels of replication would permit efficient transmission in the following active phase 24–36 h later and perhaps reduce detection at a time when the immune system is primed for pathogen attack.

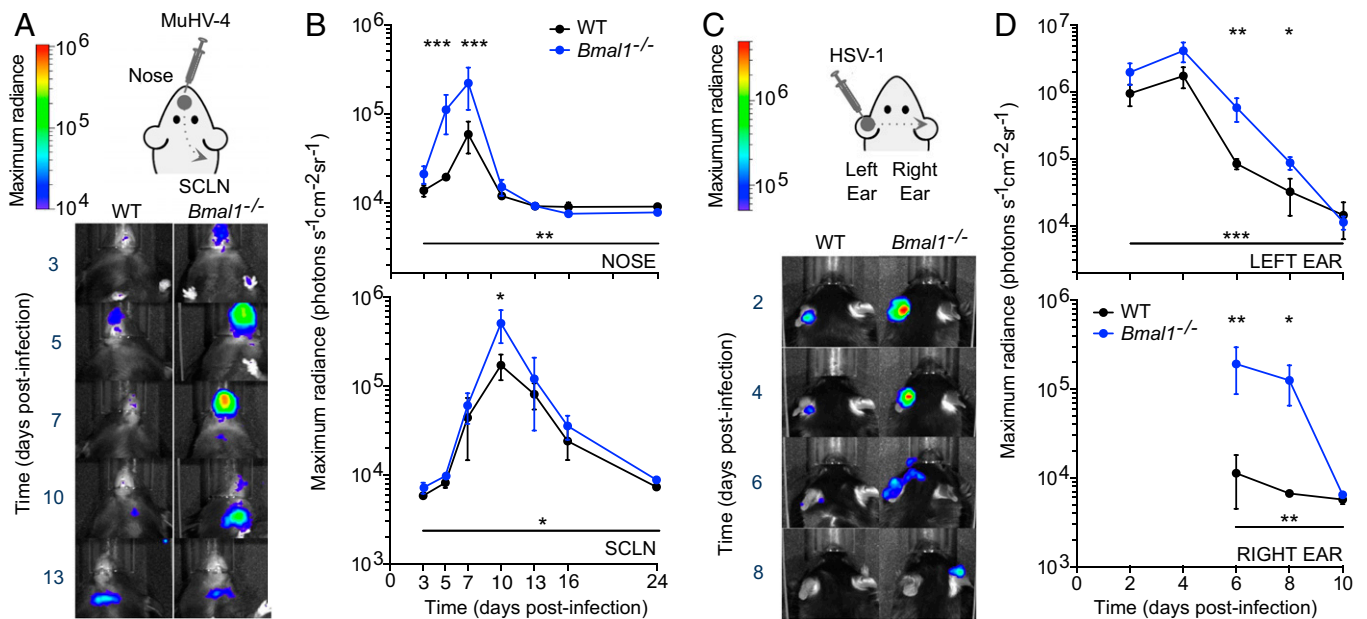


Fig. 2. Herpesvirus infection is augmented in arrhythmic *Bmal1*^{-/-} mice. (A) WT ($n = 6$) and *Bmal1*^{-/-} ($n = 5$) female mice were intranasally infected with *M3:luc* MuHV-4 at ZT7. Extent and spread of infection was monitored by bioluminescence imaging. Representative images are shown with overlaid bioluminescence radiance measurements. (B) *M3:luc* MuHV-4 progressively disseminates from the nose to the SCLNs and is significantly higher in *Bmal1*^{-/-} mice [mean \pm SEM; nose two-way ANOVA (genotype \times time postinfection): genotype effect, $P = 0.0031$; SCLN two-way ANOVA (genotype \times time postinfection): genotype effect, $P = 0.0348$; post hoc t tests: $*P < 0.05$, $**P < 0.01$, $***P < 0.001$]. See also Fig. S2A. (C) Male WT ($n = 5$) and *Bmal1*^{-/-} ($n = 6$) mice were infected with *CMV:luciferase* (*CMV:luc*) herpes simplex virus 1 (HSV-1) by scarification of the left ear at ZT7. Extent and spread of infection was monitored and images presented as for A. (D) *CMV:luc* HSV-1 progressively disseminates from the left ear to the head and right ear and is significantly higher in *Bmal1*^{-/-} mice [mean \pm SEM; left ear two-way ANOVA (genotype \times time postinfection): genotype effect, $P = 0.0004$; right ear two-way ANOVA (genotype \times time postinfection): genotype effect, $P = 0.0054$; post hoc t tests: $*P < 0.05$, $**P < 0.01$]. See also Fig. S2E.

Critically, expression of repressive clock genes, such as *mCryptochrome1* (*mCry1*) and *mPeriod2* (*mPer2*), was not induced during viral infection (Fig. 5C and Fig. S6B), but a significant, rapid reduction was seen when cells were infected at CT18 (Fig. 5C). These findings are consistent with MuHV-4 infection ushering cells from a repressive circadian phase to one where BMAL1 is active, via sustaining *Bmal1* expression and relieving CRYPTOCHROME-mediated repression. Furthermore, HSV-1 infection also acutely up-regulated *Bmal1* (Fig. 5D), even more so than MuHV-4, suggesting that *Bmal1* is specifically targeted by both α - and γ -herpesvirus families. In support of this, *Bmal1* expression is induced in cells overexpressing viral transcriptional activators from either herpesviruses (Fig. S7), and interactions between BMAL1/CLOCK and several HSV-1 transcriptional activators in vitro have been reported previously (15, 16).

Herpesviruses co-opt cellular transcriptional mechanisms to replicate and target clock transcription factors (Fig. 5). We next asked if the impact of BMAL1 ablation on viral infection extended beyond direct transcriptional regulation, to the global changes in cellular physiology that occur when circadian rhythms are disrupted. To investigate this, we infected WT and *Bmal1*^{-/-} cells with the orthomyxovirus, influenza A (IAV) (Fig. 6A and B). IAV replicates within the nucleus but encodes its own RNA-dependent RNA polymerase and therefore does not directly use the host cell's transcriptional machinery for viral gene expression, in contrast to herpesviruses. Remarkably, loss of BMAL1 also significantly augmented IAV protein expression and replication (PB2::GLUC bioluminescence two-way ANOVA: genotype effect, $P = 0.0004$; single-cycle growth two-way ANOVA: genotype effect, $P = 0.0102$). The similar impact of cellular arrhythmicity on two disparate, clinically relevant virus families implies a broader influence of circadian clocks, and specific components such as BMAL1, on viral infection.

To determine which cellular systems underpin the time-of-day effect on viral replication, we first identified proteins that exhibit changes in abundance between opposite circadian phases (CT18 vs. CT30) in WT cells, when viral replication in WT, but not in *Bmal1*^{-/-} cells, was significantly different (Fig. 4C). Given that virus infection is augmented in *Bmal1*^{-/-} cells at both time points (Fig. 4C), we then focused on the subset of proteins within this group whose abundance was either increased or decreased at both of these times in *Bmal1*^{-/-} cells compared with WT cells (Fig. 6C and D and Fig. S8). Circadian-regulated proteins expressed at higher levels in *Bmal1*^{-/-} cells were enriched for those involved in protein biosynthesis (Fig. 6C, Fig. S8A, and Table S1), including amino acid biosynthesis, ribosome structure, translation, and protein folding clusters. Additionally, proteins involved in endoplasmic reticulum function, protein localization, and intracellular vesicle trafficking were significantly enriched. These results indicate that enhanced capability for viral protein biosynthesis, assembly, and egress contribute to clock control of virus replication. Conversely, circadian-regulated proteins expressed at lower levels in *Bmal1*^{-/-} cells were enriched for those involved in organization of the cortical actin cytoskeleton and chromatin assembly (Fig. 6D, Fig. S8B, and Table S2), suggesting that virus particle uncoating, genome trafficking, and histone association contribute to clock control of virus replication. Thus, clock-mediated effects on viral infection in cells can be ascribed to discrete functional categories of protein effectors targeting specific aspects of the virus replication cycle.

Discussion

Our results show that altering only the time when hosts are infected significantly affects the extent of virus infection and dissemination in vivo, reflecting the profound change in physiology that naturally occurs over a day. Host circadian rhythms underpin this phenomenon, because behaviorally arrhythmic mice show no

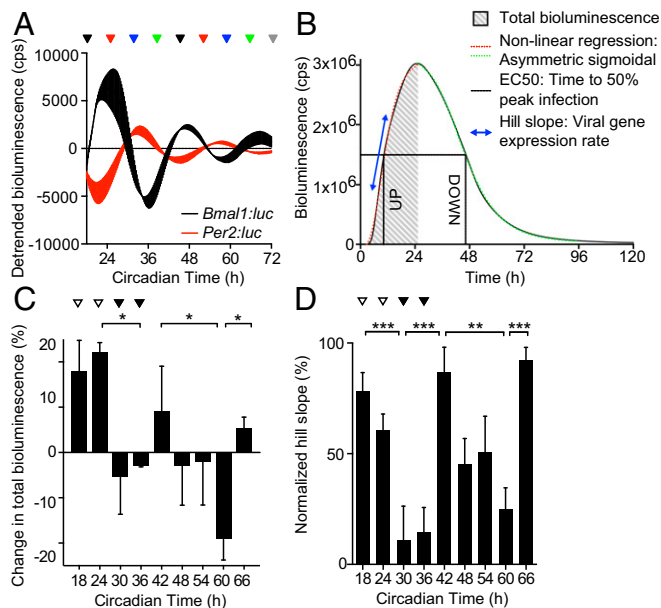


Fig. 3. Circadian rhythms modulate herpesvirus replication in cells. (A) Bioluminescence recordings from control (uninfected) temperature-synchronized *Bmal1:Luciferase* (*Bmal1:Luc*) and *Per2:Luciferase* (*Per2:Luc*) circadian reporter NIH 3T3 cells (mean \pm SEM; $n = 3$). Peak *Bmal1:Luc* bioluminescence is designated Circadian Time 24 (CT24). Colored arrows indicate circadian times (CT) at which parallel cultures of synchronized NIH 3T3 cells were infected with *M3:Luc* MuHV-4. (B) Representative bioluminescence recording and kinetic analysis parameters of *M3:Luc* MuHV-4 replication using asymmetrical sigmoidal nonlinear regression. See Fig. S4 A and B for raw bioluminescence recordings obtained from cells infected at different CTs and R^2 regression coefficients. (C) Amount of MuHV-4 replication varies significantly depending on the circadian time of infection (mean \pm SEM; $n = 3$; one-way ANOVA: total bioluminescence, $P = 0.0178$; multiple comparisons, $*P < 0.05$). Total bioluminescence calculated by the area under curve method (AUC) and normalized (0% = baseline total bioluminescence between 0 and 1 h after infection, 100% = maximum total bioluminescence value), with variation across different CTs presented as (% total bioluminescence – mean % total bioluminescence across all experimental CTs). See Fig. S4C for correlation analysis of total bioluminescence and infectious particle production (\log_{10} pfu). Open arrowheads highlight CT18/24 (higher infection) and solid arrowheads highlight CT30/36 (lower infection). (D) The rate of viral gene expression varies significantly depending on the circadian time of infection (one-way ANOVA: Hill slope, $P < 0.0001$; post hoc multiple comparisons: $**P < 0.01$, $***P < 0.001$).

such time-dependent differences. Indeed, the degree to which these intracellular pathogens replicate is a function of circadian time in isolated cells, without systemic circadian cues or host defenses.

For pathogens such as *Plasmodia*, which cause malaria, synchronizing their replication cycle with host circadian rhythms contributes to their success (17). Likewise, we speculate that coevolution of viruses with their host clocks enables them to capitalize on the predictability of daily rhythms driven by cell autonomous molecular clocks. Comparable to our findings with herpesviruses, rhythmic gene expression can persist during hepatitis C virus and influenza A virus infection, albeit with altered circadian phase and amplitude (18, 19). Whether such changes to host circadian rhythms enhance virus propagation between cells or transmission between hosts are open questions.

A key feature of cellular clocks is their ability to synchronize to external stimuli: initial time-of-day effects would be amplified if dysregulated timekeeping cues perpetuate from infected to neighboring uninfected cells. Our results strongly suggest that herpesvirus and IAV replication increases in arrhythmic cells, as demonstrated by virus-induced disruption at certain circadian

times or via loss of BMAL1. However, does this help or hinder persistence at the level of the host or population? HSV-1 disseminates more extensively in *Bmal1*^{-/-} mice, for example, but augmented primary productive replication may generate more robust adaptive immune responses.

How do viruses engage with the molecular clockwork and modulate timekeeping? At the simplest level, the circadian activity of host metabolic and trafficking pathways places constraints on replication. In turn, many viruses reprogram cellular metabolism, which can feedback directly to the core clock mechanism. A more intriguing possibility is that viruses actively gauge the cellular circadian phase via interaction with core clock components and exploit subsequent circadian variation in replication kinetics. The HSV-1 viral transactivator infected cell polypeptide 0 (ICP0) is thought to associate directly with BMAL1, whereas viral transcription is driven by a complex containing CLOCK (15, 16, 20). However, why not associate with CLOCK directly and why use BMAL/CLOCK at all? The abundance of CLOCK does not oscillate, and its circadian function is bestowed via interaction with BMAL1. We propose that herpesviruses recruit BMAL/CLOCK to lock viral transcription to cellular circadian time.

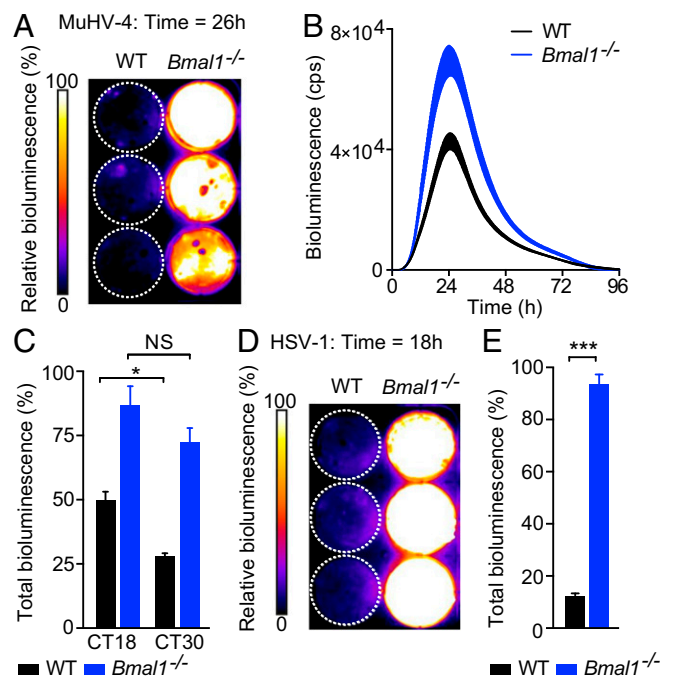


Fig. 4. Herpesvirus replication is enhanced in *Bmal1*^{-/-} cells. (A) Pseudocolored bioluminescence image of WT and *Bmal1*^{-/-} primary cells infected with *M3:Luc* MuHV-4. See also Movie S2. (B) Representative bioluminescence recordings of synchronized WT and *Bmal1*^{-/-} primary cells infected with *M3:Luc* MuHV-4 (mean \pm SEM; $n = 3$). (C) Synchronized WT and *Bmal1*^{-/-} primary cells were infected with *M3:Luc* MuHV-4 at either CT18 or CT30. MuHV-4 replication is significantly increased in *Bmal1*^{-/-} cells compared with WT cells (mean \pm SEM; $n = 3$) [total bioluminescence (AUC) normalized as for Fig. 3C; two-way ANOVA (genotype \times CT of infection): genotype effect, $P < 0.0001$]. Time-of-day effect on viral replication is observed in WT cells, but not *Bmal1*^{-/-} cells [total bioluminescence two-way ANOVA (genotype \times CT of infection): post hoc multiple comparisons: NS = not significant, $*P < 0.05$]. See Fig. S5 for circadian reporter controls and *M3:Luc* MuHV-4 kinetic analysis. (D) Pseudocolored bioluminescence image of WT and *Bmal1*^{-/-} primary cells infected with *CMV:Luc* HSV-1. See also Movie S3. (E) *CMV:Luc* HSV-1 replication is significantly increased in *Bmal1*^{-/-} cells compared with WT cells (mean \pm SEM; $n = 3$). Total bioluminescence (AUC) normalized as for Fig. 3C (two-tailed t test: $***P < 0.001$). See Fig. S4E for correlation analysis of total bioluminescence and infectious particle production (\log_{10} pfu).

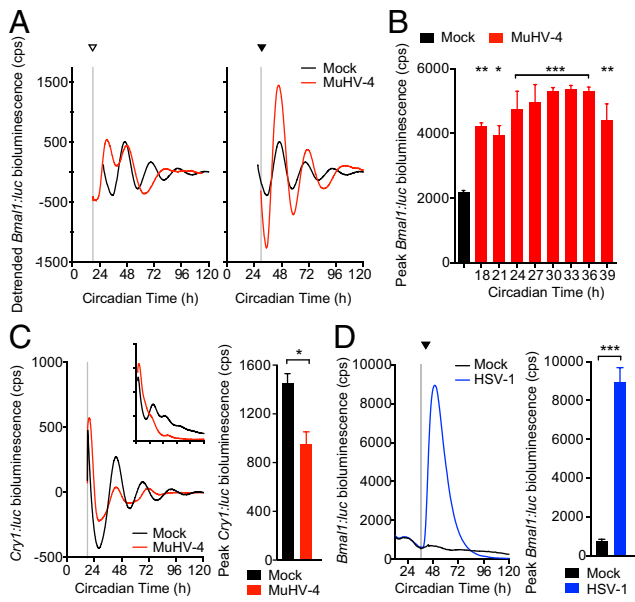


Fig. 5. Virus infection differentially affects clock gene expression. (A) Bioluminescence recordings from synchronized *Bmal1:luciferase* (*Bmal1:luc*) circadian reporter NIH 3T3 cells either mock infected or infected with MuHV-4 at CT18 (open arrowhead) and CT30 (solid arrowhead). Mean baseline-subtracted (detrended) bioluminescence ($n = 3$ per group) shown. Infection at CT18 induced an additional peak in *Bmal1:luc* expression, disrupting the circadian rhythm. Infection at CT30 induced *Bmal1:luc* expression that synergizes with circadian *Bmal1:luc* expression and preserves rhythms. (B) Peak bioluminescence from synchronized *Bmal1:luc* cells either mock infected or infected with MuHV-4 at 3-h intervals from CT18 to CT39 (mean \pm SEM; $n = 3$). *Bmal1:luc* expression is significantly increased, irrespective of the circadian time of infection (one-way ANOVA $P < 0.0001$; post hoc multiple comparisons: $*P < 0.05$, $**P < 0.01$, $***P < 0.001$). For raw bioluminescence recordings and error boundaries, see Fig. S6A. (C) Baseline-subtracted (detrended) bioluminescence traces from synchronized *mCryptochrome1:luciferase* (*Cry1:luc*) circadian reporter NIH 3T3 cells (mean; $n = 3$). (Inset) Raw bioluminescence traces (mean \pm SEM; $n = 3$). *Cry1:luc* is significantly decreased during MuHV-4 infection (postinfection peak bioluminescence two-tailed t test, $*P = 0.0188$). (D) Bioluminescence recording from synchronized *Bmal1:luc* cells mock infected or infected with HSV-1 at CT36 (solid arrowhead) (mean \pm SEM; $n = 3$). *Bmal1:luc* expression is significantly increased during HSV-1 infection (postinfection peak bioluminescence two-tailed t test, $***P < 0.001$).

We found that ICP0 induces *Bmal1* expression outside the context of infection, implying that *Bmal1* is specifically targeted, rather than a cell-intrinsic innate immune response to infection. However, this presents an apparent paradox, given that replication is enhanced in the absence of BMAL1. Why induce a protein that appears to exert an antiviral effect? Shifting cells from a repressive circadian phase via concomitant acute induction of *Bmal1* and *mCry1* repression likely stimulates replication. One straightforward explanation is that chronic arrhythmicity in *Bmal1*^{-/-} cells generates a cellular environment less equipped to deal with viral challenge or that baseline levels of BMAL1 contribute to cell intrinsic antiviral immune responses (e.g., via IFN signaling). Examining viral pathogenicity in alternate “clock knockout” genetic models and in hosts subject to chronic circadian desynchrony will help disentangle such possibilities. This apparent paradox additionally highlights the complex nature of circadian investigations, in that clock proteins may be co-opted during virus replication in ways unrelated to their timekeeping function (non-circadian effects). Therefore, the global impact of circadian rhythmicity must be considered, rather than the effect of individual clock components.

Our work does imply that constitutively low levels of BMAL1 lead to increased herpes and influenza A viral infection. Remarkably, as well as its daily oscillation, *Bmal1* expression

undergoes seasonal variation in human blood samples, with lowest levels during the winter months (21). We speculate that this may contribute to viral dissemination at the population level because many viruses, including influenza, cause infection more commonly in the winter (22). Given that global *Bmal1* expression is substantially lower in mouse models of circadian desynchronization (23), our work also suggests that shift workers might be more susceptible to viral disease and therefore prime candidates for vaccination against viruses such as influenza. Indeed, timing of influenza vaccine administration in the morning vs. afternoon

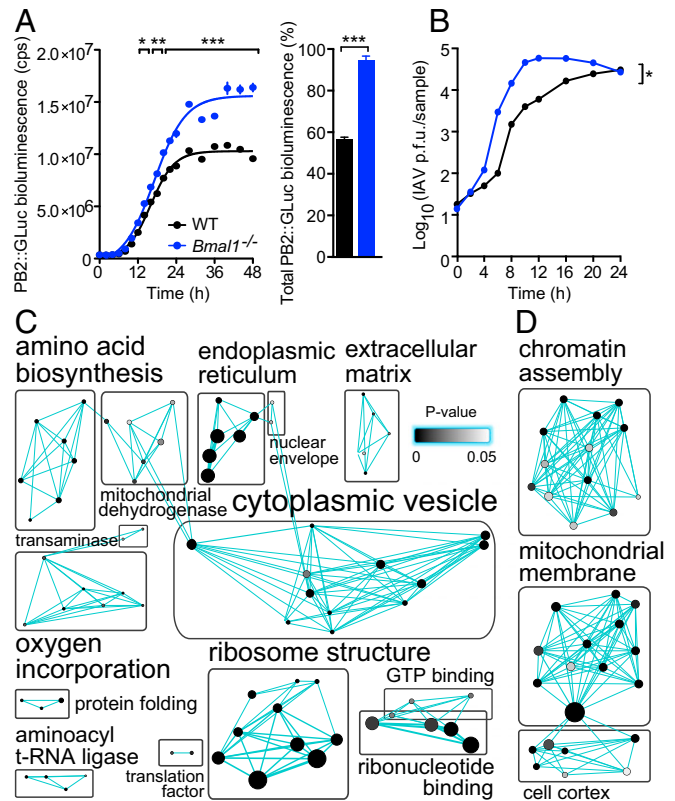


Fig. 6. Global proteomic comparison of WT and *Bmal1*^{-/-} cells reveals clock-regulated pathways that impact on viral replication. (A) Influenza A viral protein expression was enhanced in *Bmal1*^{-/-} cells. WT and *Bmal1*^{-/-} cells were infected with PB2::GLUC (*Gaussia luciferase*) influenza A virus (IAV) and luciferase activity quantified at stated intervals. Rate of PB2 expression was increased in *Bmal1*^{-/-} compared with WT cells [mean \pm SEM; $n = 3$; two-way ANOVA (genotype \times time postinfection): genotype effect, $P = 0.0004$; interaction, $P < 0.0001$; post hoc multiple comparisons: $*P < 0.05$, $**P < 0.01$, $***P < 0.001$], as was total PB2 expression (sigmoidal nonlinear regression: WT $R^2 = 0.9902$, *Bmal1*^{-/-} $R^2 = 0.9836$; total PB2::GLUC bioluminescence (AUC) two-tailed Student t test: $**P < 0.0019$). (B) Single-cycle IAV growth was enhanced in *Bmal1*^{-/-} cells. IAV-infected cells were harvested and amount of infectious IAV particles determined by plaque assay [two-way ANOVA (genotype \times time postinfection): genotype effect, $*P = 0.0102$]. (C) Synchronized WT and *Bmal1*^{-/-} primary cells were harvested at CT18 and CT30 and global proteomics performed by LC coupled to MS ($n = 3$). DAVID functional annotation clustering analysis of proteins that significantly differed at CT18 vs. CT30, and significantly increased in *Bmal1*^{-/-} cells compared with WT cells at both CT18 and CT30. Protein number represented by node size and cluster P value by node grayscale. Annotations were prescribed by the Markov cluster algorithm. Number of nodes per group represented by label size. See Fig. S8A for heat map analysis and Table S1 for enrichment scores. (D) Proteomics analysis performed as in C. DAVID functional annotation clustering analysis of proteins that significantly differed at CT18 vs. CT30 and significantly decreased in *Bmal1*^{-/-} cells compared with WT cells at both CT18 and CT30. Proteins are represented as in C. See Fig. S8B for heat map analysis and Table S2 for enrichment scores.

has recently been shown to be a determinant in the systemic immunization response in people aged >65 y (24). Beyond this, acute manipulation of the molecular circadian clockwork may provide a strategy for the development of novel antiviral therapies.

Methods

Viruses. WT MuHV-4, M50 MuHV-4 (25), *M3:luciferase* (*M3:luc*) MuHV-4 (12), WT HSV-1, and *CMV:luciferase* (*CMV:luc*) HSV-1 (13) stocks were grown in BHK21 cells and virus titer determined by plaque assay. PB2:: *Gaussia luciferase* (PB2::GLUC) influenza A virus (A/Puerto Rico/8/34 H1N1 IAV) was a kind gift from Nicholas Heaton and Peter Palese, Icahn School of Medicine at Mount Sinai, New York (26). *SI Methods* provides further details.

Mice. Animal experimentation was licensed by the Home Office under the Animals (Scientific Procedures) Act 1986, with University of Cambridge Local Ethical Review. Animals had ad libitum access to chow and water and were maintained on 12-h light:12-h dark cycles, with lights on and lights off designated ZT0 and ZT12, respectively. At stated ZTs, age-matched C57BL/6J WT (*Bmal1^{+/+}*) and *Bmal1^{-/-}* mice were intranasally infected with 1×10^4 plaque-forming units (pfu) *M3:luc* MuHV-4 or 5×10^5 pfu *CMV:luc* HSV-1 by left ear scarification. Bioluminescence imaging was performed with an IVIS Lumina and analyzed using Living Image software (Caliper Life Sciences). See *SI Methods* for further details.

Cell Culture and Bioluminescence Assays. Primary fibroblasts were generated as described previously (27). Circadian transcriptional rhythms were monitored using confluent NIH 3T3 fibroblasts (ATCC) transfected with *mPeriod2:luciferase*, *mCryptochrome1:luciferase*, or *Bmal1:luciferase* reporters and temporally synchronized by temperature cycles (32 °C:37 °C; 12 h:12 h) or 100 nM dexamethasone treatment (28). For comparison between in vivo and in vitro experiments, peak *Bmal1:luc* bioluminescence was operationally designated as CT = 0/24 h. *M3:luc* MuHV-4 and *CMV:luc* HSV-1 infections were performed at high multiplicity of infection (MOI = 1–3 pfu/cell). Bioluminescence was monitored using a LumiCycle-32 system (Actimetrics) or Alligator Bioluminescence Incubator System (Cairn Research). PB2::GLUC IAV (MOI = 2 pfu/cell) replication was assessed by sampling medium at intervals postinfection and determining *Gaussia*

luciferase activity using a BioLux Kit (NEB E3300L). See *SI Methods* for further details.

Proteomics. Synchronized, confluent primary WT and *Bmal1^{-/-}* cells were harvested at either CT = 18 h or CT = 30 h. Lysates were digested and labeled with tandem mass tags (TMTs) according to the manufacturer's instructions (Thermo). Peptide mixtures were separated on a 50-cm, 75- μ m-ID Pepmap column over a 3-h gradient at 40 °C and eluted directly into the mass spectrometer (Thermo Q Exactive Orbitrap). Xcalibur software was used to control the data acquisition. MaxQuant v1.5.2.8 was used to process the raw data acquired with a reporter ion quantification method (29). The Uniprot KB database of mouse sequences was used for peptide identification [false discovery rate (FDR) = 0.1%]. Two-tailed t tests were performed in Perseus (FDR cutoff = 0.05; within-groups variance S_0 factor = 0.1) to identify proteins significantly different between CT18 and CT30 in WT cells, but not *Bmal1^{-/-}* cells. This group was then tested via two-tailed t test for significant differences between WT and *Bmal1^{-/-}* cells at both CT18 and CT30 (FDR cutoff = 0.05), presented graphically in R using the HeatMap package and subject to Database for Annotation, Visualization and Integrated Discovery (DAVID) functional annotation clustering analysis. Outputs were graphically presented using Cytoscape EnrichmentMap and annotated using Cluster-maker Markov Cluster Algorithm and WordCloud (30, 31). See *SI Methods* for further details.

Statistical Analysis. Unless otherwise stated, statistical analysis was performed using Prism (GraphPad Software). Bioluminescence data were analyzed using LumiCycle Data Analysis software (Actimetrics). See *SI Methods* for further details.

ACKNOWLEDGMENTS. We thank L. Ansel-Bollepalli and I. Robinson for animal assistance; A. Snijders, H. Flynn (Francis Crick Institute Proteomics Core), and S. Ray for assistance with proteomics data analysis; N. Heaton, P. Palese (Icahn School of Medicine at Mount Sinai), and A. Miyawaki (RIKEN Brain Science Institute, Japan) for Fucci2 lentiviral vectors; and H. Coleman and M. Jain for helpful discussions. A.B.R. acknowledges funding from the Wellcome Trust (Grants 083643/Z/07/Z, 100333/Z/12/Z, and 100574/Z/12/Z), the European Research Council (Grant 281348, MetaCLOCK), the European Molecular Biology Organization Young Investigators Programme, the Lister Institute of Preventative Medicine, and the Medical Research Council (MRC_MC_UU_12012/5). A.D.N. acknowledges Marie Curie Actions (FP7/2007-2013; Research Executive Agency Grant Agreement 627630).

1. Takahashi JS, Hong HK, Ko CH, McDearmon EL (2008) The genetics of mammalian circadian order and disorder: Implications for physiology and disease. *Nat Rev Genet* 9(10):764–775.
2. Bunker MK, et al. (2000) Mop3 is an essential component of the master circadian pacemaker in mammals. *Cell* 103(7):1009–1017.
3. van der Horst GT, et al. (1999) Mammalian Cry1 and Cry2 are essential for maintenance of circadian rhythms. *Nature* 398(6728):627–630.
4. O'Neill JS, Maywood ES, Hastings MH (2013) Cellular mechanisms of circadian pacemaking: Beyond transcriptional loops. *Handbook Exp Pharmacol* (217):67–103.
5. Scheiermann C, Kunisaki Y, Frenette PS (2013) Circadian control of the immune system. *Nat Rev Immunol* 13(3):190–198.
6. Curtis AM, Bellet MM, Sassone-Corsi P, O'Neill LA (2014) Circadian clock proteins and immunity. *Immunity* 40(2):178–186.
7. Gibbs JE, et al. (2012) The nuclear receptor REV-ERB α mediates circadian regulation of innate immunity through selective regulation of inflammatory cytokines. *Proc Natl Acad Sci USA* 109(2):582–587.
8. Nguyen KD, et al. (2013) Circadian gene Bmal1 regulates diurnal oscillations of Ly6C (hi) inflammatory monocytes. *Science* 341(6153):1483–1488.
9. Koike N, et al. (2012) Transcriptional architecture and chromatin landscape of the core circadian clock in mammals. *Science* 338(6105):349–354.
10. Bass J, Takahashi JS (2010) Circadian integration of metabolism and energetics. *Science* 330(6009):1349–1354.
11. Stevenson PG, Efsthathiou S (2005) Immune mechanisms in murine gammaherpesvirus-68 infection. *Viral Immunol* 18(3):445–456.
12. Milho R, et al. (2009) In vivo imaging of murine herpesvirus-4 infection. *J Gen Virol* 90(Pt 1):21–32.
13. Shivkumar M, et al. (2013) Herpes simplex virus 1 targets the murine olfactory neuroepithelium for host entry. *J Virol* 87(19):10477–10488.
14. Zhang R, Lahens NF, Ballance HI, Hughes ME, Hogenesch JB (2014) A circadian gene expression atlas in mammals: Implications for biology and medicine. *Proc Natl Acad Sci USA* 111(45):16219–16224.
15. Kawaguchi Y, et al. (2001) Herpes simplex virus 1 alpha regulatory protein ICP0 functionally interacts with cellular transcription factor BMAL1. *Proc Natl Acad Sci USA* 98(4):1877–1882.
16. Kalamvoki M, Roizman B (2011) The histone acetyltransferase CLOCK is an essential component of the herpes simplex virus 1 transcriptome that includes TFIIID, ICP4, ICP27, and ICP22. *J Virol* 85(18):9472–9477.
17. O'Donnell AJ, Schneider P, McWatters HG, Reece SE (2011) Fitness costs of disrupting circadian rhythms in malaria parasites. *Proc Biol Sci* 278(1717):2429–2436.
18. Benegiamo G, et al. (2013) Mutual antagonism between circadian protein period 2 and hepatitis C virus replication in hepatocytes. *PLoS One* 8(4):e60527.
19. Sundar IK, et al. (2015) Influenza A virus-dependent remodeling of pulmonary clock function in a mouse model of COPD. *Sci Rep* 4:9927.
20. Kalamvoki M, Roizman B (2010) Circadian CLOCK histone acetyl transferase localizes at ND10 nuclear bodies and enables herpes simplex virus gene expression. *Proc Natl Acad Sci USA* 107(41):17721–17726.
21. Dowell SF (2001) Seasonal variation in host susceptibility and cycles of certain infectious diseases. *Emerg Infect Dis* 7(3):369–374.
22. Dopico XC, et al. (2015) Widespread seasonal gene expression reveals annual differences in human immunity and physiology. *Nat Commun* 6:7000.
23. Filipiński E, et al. (2005) Effects of light and food schedules on liver and tumor molecular clocks in mice. *J Natl Cancer Inst* 97(7):507–517.
24. Long JE, et al. (2016) Morning vaccination enhances antibody response over afternoon vaccination: A cluster-randomised trial. *Vaccine* 34(24):2679–2685.
25. May JS, Coleman HM, Smillie B, Efsthathiou S, Stevenson PG (2004) Forced lytic replication impairs host colonization by a latency-deficient mutant of murine gammaherpesvirus-68. *J Gen Virol* 85(Pt 1):137–146.
26. Heaton NS, et al. (2013) In vivo bioluminescent imaging of influenza A virus infection and characterization of novel cross-protective monoclonal antibodies. *J Virol* 87(15):8272–8281.
27. Seluanov A, Vaidya A, Gorbunova V (2010) Establishing primary adult fibroblast cultures from rodents. *J Vis Exp* (44):e2033.
28. Nagoshi E, et al. (2004) Circadian gene expression in individual fibroblasts: Cell-autonomous and self-sustained oscillators pass time to daughter cells. *Cell* 119(5):693–705.
29. Tusher VG, Tibshirani R, Chu G (2001) Significance analysis of microarrays applied to the ionizing radiation response. *Proc Natl Acad Sci USA* 98(9):5116–5121.
30. Merico D, Isserlin R, Stueker O, Emili A, Bader GD (2010) Enrichment map: A network-based method for gene-set enrichment visualization and interpretation. *PLoS One* 5(11):e13984.
31. Lopes CT, et al. (2010) Cytoscape Web: An interactive web-based network browser. *Bioinformatics* 26(18):2347–2348.
32. Sakaue-Sawano A, et al. (2008) Visualizing spatiotemporal dynamics of multicellular cell-cycle progression. *Cell* 132(3):487–498.
33. Coleman HM, et al. (2008) Histone modifications associated with herpes simplex virus type 1 genomes during quiescence and following ICP0-mediated de-repression. *J Gen Virol* 89(Pt 1):68–77.